Journal of Applied Polymer Science

Effect of SiO_2 and TiO_2 nanoparticle on the properties of phenyl silicone rubber

Huan Yang,[1] Qun Gao,[1] Yunting Xie,[2] Qian Chen,[1] Chunfa Ouyang,[1] Yaomin Xu,[1] Xiaoting Ji[1]
[1]School of Materials Science & Engineering, Shanghai Institute of Technology, Shanghai 201418, China
[2]School of Materials Science & Engineering, Shanghai University, Shanghai 200444, China
Correspondence to: Q. Gao (E-mail: wityy@sit.edu.cn)

ABSTRACT: Two types of nanoparticles TiO_2 and SiO_2 treated with silane coupling agents were incorporated into phenyl silicone rubber at a low concentration ($\leq$1.0%) and cured by the room temperature vulcanized method. The results showed that treated TiO_2 or SiO_2 nanoparticles improved the ultraviolet (UV)-shielding ability and enhanced the visible transmittance of the phenyl silicone rubber, compared with their respective untreated particles. Moreover, when comparing treated nanoparticles, TiO_2 was more responsible for augmenting the UV-shielding ability of the phenyl silicone rubber, while SiO_2 played a more important role in increasing the transmittance of visible light. Low levels of nanoparticles reduced the dielectric constant of the nanocomposite; however, on reaching a critical concentration, increasing the nanoparticle content had the opposite effect. The thermal conductivity of nanocomposites increased linearly with the amount of treated nanoparticles, while SiO_2 nanocomposites exhibited better thermal conductivity than those of TiO_2. © 2015 Wiley Periodicals, Inc. J. Appl. Polym. Sci. **2015**, *132*, 42806.

KEYWORDS: grafting; nanoparticles; nanowires and nanocrystals; optical properties; rubber; thermal properties

Received 15 March 2015; accepted 4 August 2015
DOI: 10.1002/app.42806

INTRODUCTION

Phenyl silicone rubber is an important silicone-based material, which is formed by introducing a phenyl group onto the main chain of dimethyl silicone rubber. Low-temperature flexibility and excellent resistance to oxidation and radiation make this class of materials an attractive candidate for use in outdoor applications.[1]

Large-scale implementation of silicone rubber in many industries is restricted because of its low mechanical properties (tensile strength), and considerable efforts have been directed toward improving these properties. On one hand, chemical modifications have been attempted, such as replacing some of the methyl groups of poly(dimethylsiloxane) with vinyl groups or adding phenylene to the main chain. On the other hand, physical methods have been attempted such as functionalized fumed silica and nonreactive polyhedral oligomeric silsesquioxane into the silicone matrix[2] or combining sol–gel particles (e.g., nanosilica) with liquid silicone rubber. The main function of fillers reinforcement is to enhance adhesion strength, tensile strength, modulus, or abrasion resistance.[3,4]

Particulate-filled polymers are often classified as either microcomposites or nanocomposites, depending on the dimensions of the smallest phase-separated region. The properties of composites are often strongly influenced by very low volume fractions of nanoparticles. These phenomena are mainly attributed to the nanoeffect that leads to changes in the interphase and morphology of these systems. Currently, nanoparticles of SiO_2, ZnO, carbon black, $BaTiO_3$, Al_2O_3, and lead zirconate titania are widely used in the silicone rubber industry to improve mechanical, dielectric, and optical properties.[5–9] However, unmodified nanoparticles tend to aggregate because of strong cohesive forces and poor mixing with polymers. Under these conditions, the nanoparticle/polymer composites often display poor mechanical and dielectric properties, for example, the electrical breakdown strength of these materials always decreased and could only be used at low electrical fields.[10] Developing more favorable interfacial interactions between nanoparticles and the polymer matrix would lead to greater dispersity and result in the improvement of the mechanical and dielectric properties of the composites.

To date, silica structures have been the most widely used material to reinforce industrial silicone elastomers, as they can simultaneously offer a high structural resemblance (compatibility), an improved stress bearing ability, a higher heat tolerance and most importantly higher optical transmissibility.[11–15] Meanwhile, among various materials, TiO_2 is one of the more promising candidates because of its high refractive index ($n = 2.5$ for

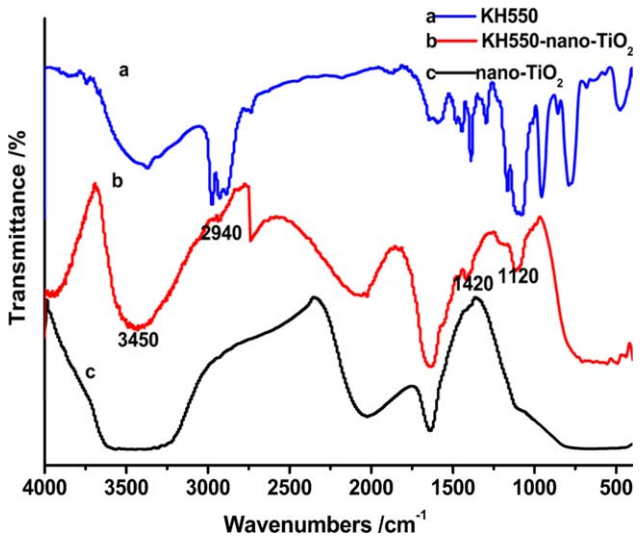

Figure 1. FTIR spectra of nano-TiO_2 and nano-TiO_2 treated with KH-550. [Color figure can be viewed in the online issue, which is available at wileyonlinelibrary.com.]

anatase phase), high dielectric constant (48), low absorption in the visible region, and dispersibility in silicone.[6,16–18]

Little research exists that has focused on comparing the effects of TiO_2 and SiO_2 nanoparticles on the physical and chemical comparison of the effects of TiO_2 and SiO_2 nanoparticles on the physics and chemistry properties of room temperature vulcanized (RTV) phenyl silicone rubber at low concentration ($\leq$1.0%).

In this article, TiO_2 and SiO_2 were treated with silane coupling agents and used to prepare nanoparticle/polymer composites by the RTV method. The effects of the two types of nanoparticles on optical transmittance, thermal conductivity, and dielectric behavior of phenyl silicone rubber composites were investigated.

MATERIALS AND METHODS

Materials

Polydimethyldiphenylsiloxane (PDMDPS) was purchased from Shanghai Resin Factory, China. The SiO_2 and TiO_2 (anatase) used in this study were supplied by Beijing DK Nano Technology, China. The average particle size of SiO_2 was 20–30 nm, while that of TiO_2 was approximately 10 nm. Ethyl silicate, dibutyltin dilaurate, absolute ethanol, and 3-(triethoxysilyl)-1-propanamine (KH550) were purchased from Sinopharm Chemical Reagent, China.

Surface Modification of SiO_2 and TiO_2 Nanoparticles

The nanoparticles were kept at 80 °C and under vacuum for 3 h to remove air and moisture. Absolute ethanol and KH550 were added to the nanoparticles and the mixture was ultrasonicated for 20 min to aid in dispersion. The mixture was then refluxed while it was stirred at 80 °C for 3 h. The resultant mixture was centrifuged and then washed with absolute ethanol to remove residual KH550. The nanoparticles were dried in a vacuum oven at 120 °C for 24 h, forming the treated filler.

Preparation of Nanoparticles/Phenyl Silicone Rubber Nanocomposites

The treated filler particles were dispersed in moderate absolute ethanol and ultrasonicated for 20 min. The PDMDPS was added to the solution and mixed uniformly. The mixtures were then conditioned in a vacuum oven for 2 h at 80 °C to remove the solvent. The composite (100 parts by weight) was mixed with ethyl silicate (crosslinking agent; 5 parts by weight) and dibutyltin dilaurate (catalyst; 2 parts by weight). The mixtures were conditioned in a vacuum oven for 30 min, to remove air bubbles generated during mixing, and then cured at room temperature for 2 days.

Characterization

The transmittance of nanocomposites was characterized by a ultraviolet visible (UV–Vis) spectrophotometer (APL instrument, 754N, China) at a wavelength of 200–1000 nm.

The thermogravimetric analysis (TGA) was investigated from 30 to 800 °C with a heating rate of 10 °C/min using a thermogravimetric analyzer (PerkinElmer, TGA-7, America) under nitrogen atmosphere.

The mechanical strengths (tensile strength, elongation) of the cured silicone rubber were characterized using a tensile tester (GALDABINI, SUN500, Italy) at room temperature.

Sample dimensions and testing procedure were in accordance with DIN 53504-1994. The crosshead speed was 50 mm/min. All measurements were repeated six times and the values averaged.

Dielectric property measurements were characterized by high-frequency Q meter (Wuyi electronics, QBG-3, China).

The dielectric constant of specimens was measured using a fixed frequency of 800 KHz at the room temperature.

The volume resistivity of the treated RTV silicone rubber was measured by resistance meter (Inesa instrument, ZC36, China). The sample has a dimension of 70–90 mm and the thickness of 2 mm.

The transmission electron microscope (TEM) images were taken with a JEOL JEM-2100 microscope operated at an acceleration voltage 200 kV.

RESULTS AND DISCUSSION

Surface Modification and Grafting Amount of SiO_2/TiO_2 Nanoparticles

Figure 1 shows the FTIR spectra of KH550, KH550 treated nano-TiO_2, and nano-TiO_2 alone. The main peaks characteristic of nano-TiO_2 (curve c) are assigned as follows: the band at 3450 cm^{-1} is attributed to the Ti—OH stretching mode, and the band at 500–800 cm^{-1} is associated with the Ti—O stretching mode. As indicated in Figure 1(curve b), the main peaks characteristic of KH550-nano-TiO_2 are assigned as follows: the bands at 1470 and 2930 cm^{-1} are attributed to —CH_2— bending and stretching modes. The band at 1560 cm^{-1} is designated as the —NH_2 bending mode.

Figure 2 shows the FTIR spectra of KH550 treated nano-SiO_2 and untreated nano-SiO_2. The spectrum of nano-SiO_2 has strong absorption bands related to Si—O—Si and Si—OH

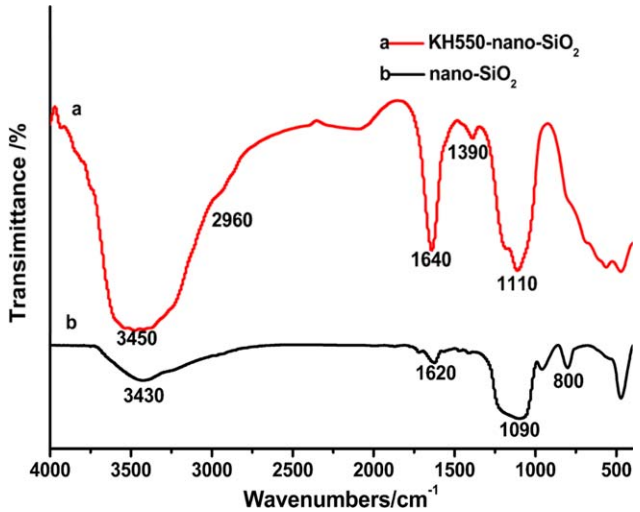

Figure 2. FTIR spectra of nano-SiO_2 and nano-SiO_2 treated with KH-550. [Color figure can be viewed in the online issue, which is available at wileyonlinelibrary.com.]

absorptions (1110 cm^{-1}, 800 cm^{-1}, and 3430 cm^{-1}), and the band at 1620 cm^{-1} is attributed to absorbed water (Figure 2, curve b). Curve a indicates that the main peaks characteristic of KH550-nano-SiO_2 are assigned as follows: the bands at 1390 and 2960 cm^{-1} are attributed to —CH_3 bending and stretching modes, the bands at 3450 cm^{-1} and 1640 cm^{-1} are attributed to —OH stretching mode and absorbed water at 3450 cm^{-1} and 1640 cm^{-1}, respectively.

TGA was used to evaluate the amount of coupling agent that was grafted to the surface of the nanoparticles. TGA analyses were performed from 30 to 800 °C under a nitrogen atmosphere. The results are displayed in Figure 3.

From Figure 3(curve a), it can be observed that the residual weight of pure nano-TiO_2 is greater than that of KH550/TiO_2. This observation can be attributed to the weight loss of the coupling agent. Similar results were obtained from the TGA of SiO_2 and KH550/SiO_2.

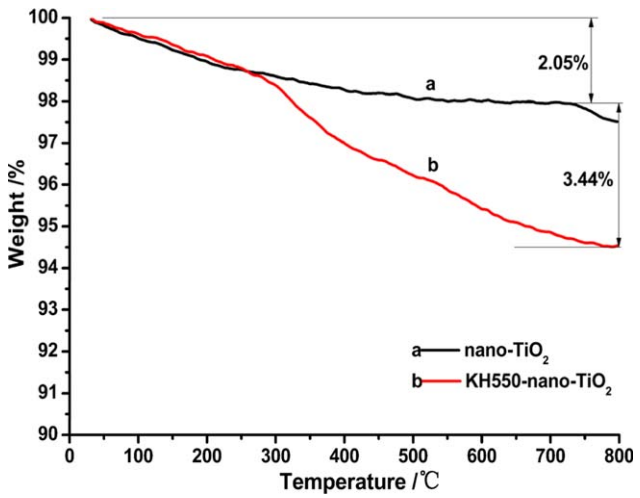

Figure 3. The TGA curves for nano-TiO_2 and nano-TiO_2 treated with KH-550. [Color figure can be viewed in the online issue, which is available at wileyonlinelibrary.com.]

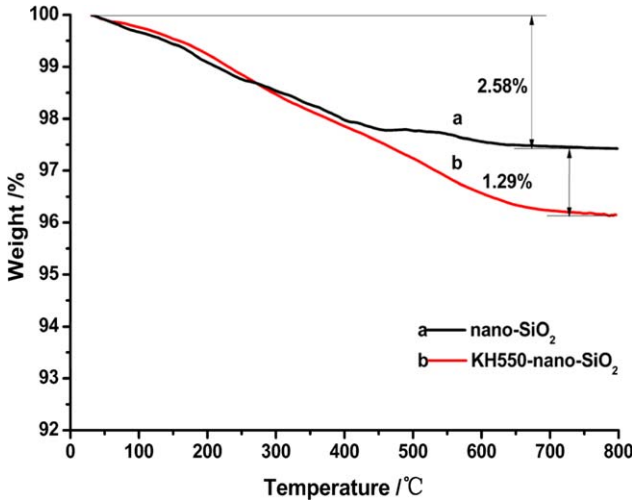

Figure 4. The TG curves of nano-SiO_2 and nano-SiO_2 treated with KH-550. [Color figure can be viewed in the online issue, which is available at wileyonlinelibrary.com.]

The weight loss process of nanoparticle TiO_2 is changed upon being treated with the coupling agent. The untreated particles show comparably higher weight loss at a lower temperature (100–300 °C). However, the treated particles show more weight loss above 300 °C. These results indicate that the surfaces of the treated particles are hydrophobic and that the adsorbed water content is less than for the native nanoparticles. Figure 3(curve a) shows a maximum weight loss of 2.05% for temperatures up to 800 °C that is attributed to both physisorbed and chemisorbed water on the surface of TiO_2 nanoparticles. The TGA curve of modified TiO_2 nanoparticles shows a weight loss of 5.49% up to 800 °C because of the oxidative thermal decomposition of KH-550 chains. As shown in Figure 3(curve c), the difference in weight loss at 800 °C between TiO_2 and treated TiO_2 nanoparticles reveals that the silane coupling agent grafting amount is approximately 3.44%.

Figure 4 shows the TGA curves of SiO_2 and treated SiO_2 nanoparticles. The TGA curve of modified SiO_2 nanoparticles shows a weight loss of 3.87% for temperatures up to 800 °C. By subtracting the weight loss of untreated particles, the weight loss caused exclusively by the grafting of KH550 was calculated, and it was revealed that the grafting amount of SiO_2 nanoparticles is approximately 1.29%.[19]

The Morphology of the Nanoparticles Dispersed in Phenyl Silicone Rubber

Figure 5(curve a–h) presents TEM micrographs of treated and untreated nanoparticles at a concentration of 0.06 wt % in phenyl silicone rubber. The nanoparticles are clearly visible as dark colored regions in the silicone rubber matrix. Figure 5(curve a–d) are TEM micrographs of treated and untreated SiO_2 nanocomposites. These images show that, after modification, nano-SiO_2 disperses homogenously in the silicone matrix, and that the diameters of the silica particles are in the range of 7–20 nm (Figure 5, curve b). However, the diameter of SiO_2 in the

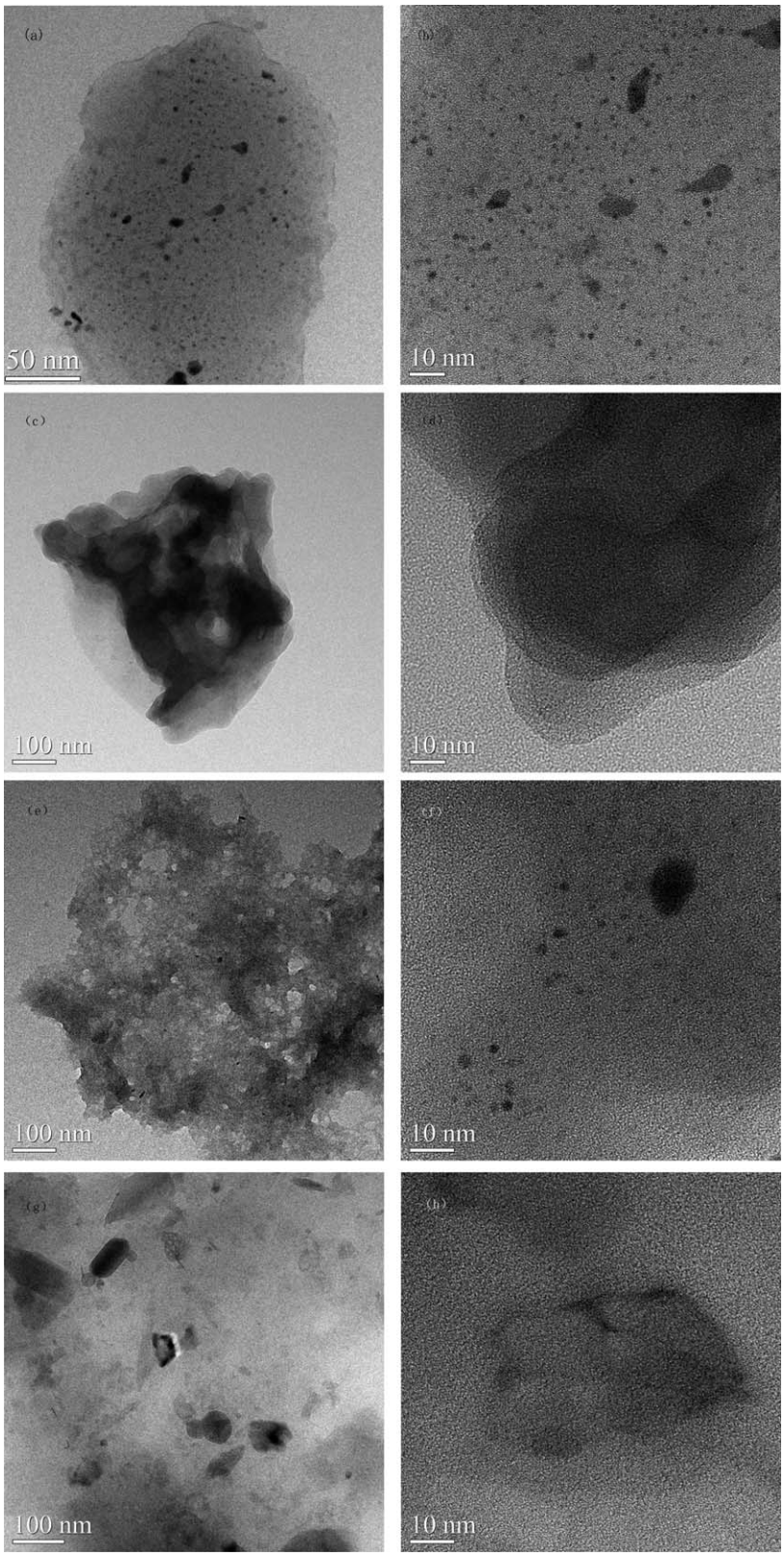

Figure 5. TEM images of treated SiO_2 (a, b), untreated SiO_2 (c, d), treated TiO_2 (e, f) and untreated TiO_2 (g, h) at a nanoparticle concentration of 0.06 wt % in the phenyl silicone rubber matrix.

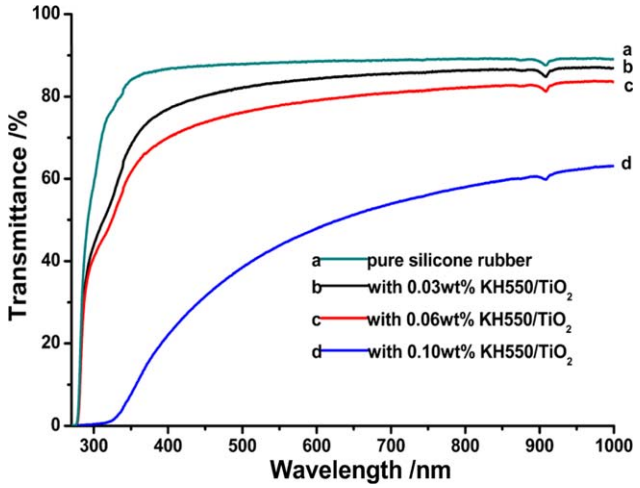

Figure 6. The transmittance of nanocomposites with various nano-TiO2 concentrations. [Color figure can be viewed in the online issue, which is available at wileyonlinelibrary.com.]

silicone rubber is more than 20 nm. The SiO_2 reveal a uniform shape where the particle morphology is spherical. Figure 5(curve e–h) shows that, while embedded in the silicone matrix, the treated nano-TiO_2 is homogenous with a mean particle diameter of 10 nm. However, the untreated TiO_2 exhibits a less homogeneous dispersion and varied in size from 20 nm to 50 nm. From the TEM images, it is clear that, after modification, the average particle size decreases and the nanoparticle distribution becomes more uniform.

Effects of SiO_2 and TiO_2 Nanoparticles on the Transmittance of Phenyl Silicone Rubber

The transmittances of the phenyl silicone rubber mixed with various concentrations of nanoparticles are shown in Figures 6 and 7.

As observed from Figure 6, the transmittances of nanocomposites decrease significantly with increasing TiO_2 concentration. In the UV range (200 nm–400 nm), the light loss is substantial for all nanocomposites, which is because of the absorption range of TiO_2 fillers. The band gap for TiO_2 (anatase) is 3.2 eV, corresponding to the absorption edge at 388 nm.[20] Illumination of TiO_2 by light with energy greater than its band gap, that is, with a wavelength shorter than the absorption edge, results in the promotion of electrons from the valance band to the conduction band. The absorption in the visible region (400–800 nm) for a TiO_2 concentration below 0.1 wt %, is negligible because the electrons do not absorb sufficient energy to transition to the conduction band. However, Rayleigh scattering that originates from the mismatch between the refraction index of TiO_2 particles (2.5)[21] and the phenyl silicone rubber matrix (1.5) may reduce visible transmission.

The transmittances of phenyl silicone rubber blends with various concentration of treated SiO_2 are shown in Figure 7. The visible transmittance of silicone rubber mixed with treated SiO_2 nanoparticles at concentrations below 1% is higher than the untreated material. The effect of SiO_2 nanoparticles on the transmittance of phenyl silicone rubber is dependent upon the wavelength. There are a series of intersections between the pure phenyl silicone rubber and the rubber with different loadings of SiO_2 0.06 wt %, 0.1 wt % and 0.6 wt % and 1.0 wt %, located in Figure 7 at A, B, C, and D, respectively. The treated SiO_2 nanocomposites possess a higher UV absorption when compared to the pure phenyl silicone rubber before the intersection of the two spectra. After the intersection, the transmittance of the treated SiO_2 nanocomposites is higher than that observed for pure phenyl silicone rubber. This phenomenon illustrates that the phenyl silicone rubber with treated nanoparticles absorbed UV-light and can improve the visible transmittance of phenyl silicone rubber. The difference in transparency between pure silicone rubber and treated SiO_2 nanocomposites is explained by the degree of light scattering. When light scattering caused by dispersed spherical particles occurs in the obtained SiO_2/silicone rubber composites, transmittance is described as in eq. (1)

$$\frac{I}{I_0} = \exp\left[-\frac{3V_p x r^3}{4\lambda^2}\left(\frac{n_p}{n_m}-1\right)\right] \quad (1)$$

in which I is the output light intensity, I_0 is the incident light intensity, x is the optical path length, V_p is the particle volume fraction, r is the particle radius, λ is the light wavelength, and

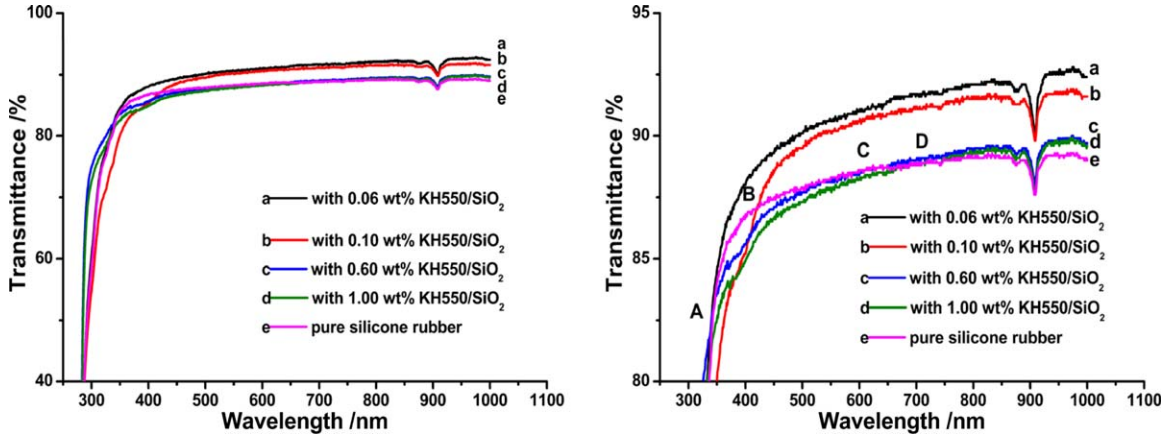

Figure 7. The transmittance of nanocomposites with various nano-SiO2 concentrations. [Color figure can be viewed in the online issue, which is available at wileyonlinelibrary.com.]

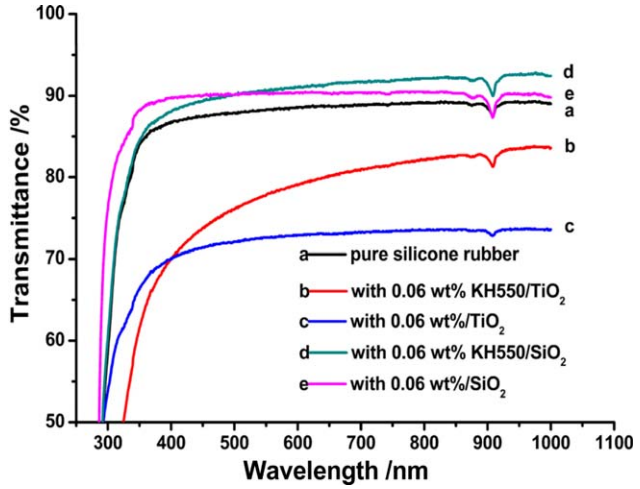

Figure 8. The transmittances of the phenyl silicone rubber blends with SiO_2 and TiO_2. [Color figure can be viewed in the online issue, which is available at wileyonlinelibrary.com.]

n_p and n_m are the refractive index of the particles and matrices, respectively.[22] In this UV/Vis measurement, because the thickness of each composite was set to be 2 mm, the optical path length (x) is treatable as a constant. Since the refractive index of nano-SiO_2 (1.46) is similar to the silicone rubber matrix (1.50), and the particles size of treated SiO_2 presented much smaller than the visible wavelength, thus leading to much higher transparency.

Figure 8 provides a comparison of the transmittances of phenyl silicone rubber blends with both treated and untreated SiO_2 and TiO_2 nanoparticles. It is evident that the transmittance of treated TiO_2 and SiO_2 nanocomposites in the UV is lower than the untreated ones. This implies that the TiO_2 treated with coupling agent can increase the UV-shielding property of phenyl silicone rubber. However, for visible wavelengths, the transmittance of phenyl silicone rubber with treated TiO_2 is apparently higher than the untreated nanocomposite. In addition, the treated SiO_2 can increase the transmittance of visible light of phenyl silicone rubber. These characteristics are consistent with the demands of a light emitting diode encapsulant, which maintains a high transmittance in visible light region and has a high absorptivity for UV-light.

Effect of SiO_2/TiO_2 Nanoparticles on the Dielectric Behavior of Phenyl Silicone Rubber

The dielectric property of the composites depends on the volume fraction, size and shape of the conducting filler. It would also be affected by other factors such as the method of composite preparation and the interface that forms as a result of the interaction between the fillers and the polymer.[23–25]

Figure 9 shows the dependencies of the dielectric constant at 800 KHz on the mass fraction of TiO_2 and SiO_2, and a decrease of the dielectric constant is observed at low mass fractions.

This property is attributed to the nanoparticles hindering the movement of silicone molecular chains and, thereby, decreasing the polarizability of the polymer matrix.[26,27] The increase in dielectric constant at higher mass fractions is attributed to the dielectric confinement effect.

The volume resistivity (ρ_v) of phenyl silicone rubber with different mass fractions of TiO_2 and SiO_2 is shown in Figure 10. The volume resistivity gradually increases with the nanoparticle concentration up to 1 wt %. This phenomenon might be ascribed to electrode polarization and the interface polarization between nanoparticle and phenyl silicone rubber phases, given that the formation of interfacial regions is directly related to increasing nanoparticle content. The primary factors influencing the resistivity of a composite are the interfacial interactions that produce energy barriers and block the transport of electrons.[7] For treated TiO_2 and SiO_2 nanoparticles, which were tightly combined with the rubber matrix, there is a tunneling barrier restricting electrons attempting to transfer from the polymer to the nanoparticle. Moreover, because of the modification of SiO_2 and TiO_2 fillers, the effect of electron tunneling is greatly

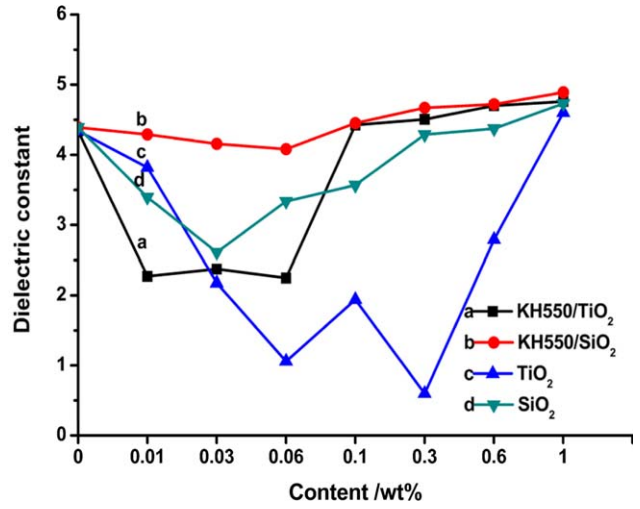

Figure 9. The effect of TiO_2 and SiO_2 content on the dielectric constant of silicone composites under 800 KHz. [Color figure can be viewed in the online issue, which is available at wileyonlinelibrary.com.]

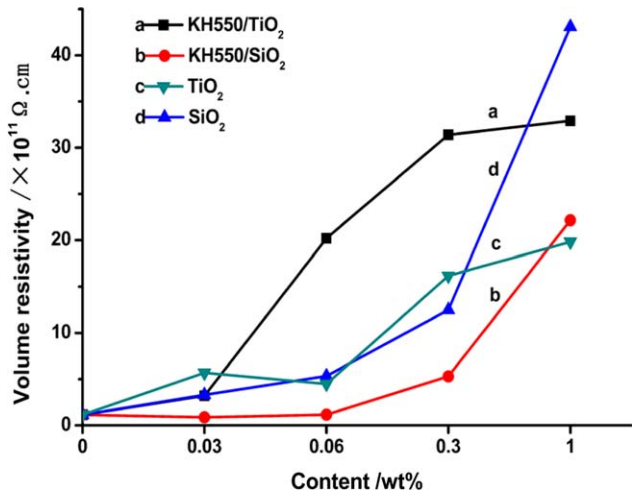

Figure 10. The effect of TiO_2 and SiO_2 content on volume resistivity of silicone composites. [Color figure can be viewed in the online issue, which is available at wileyonlinelibrary.com.]

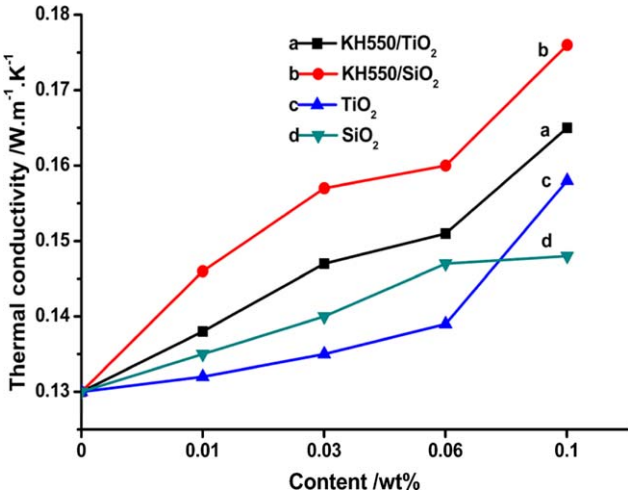

Figure 11. The effect of TiO_2 and SiO_2 content on thermal conductivity of silicone composites. [Color figure can be viewed in the online issue, which is available at wileyonlinelibrary.com.]

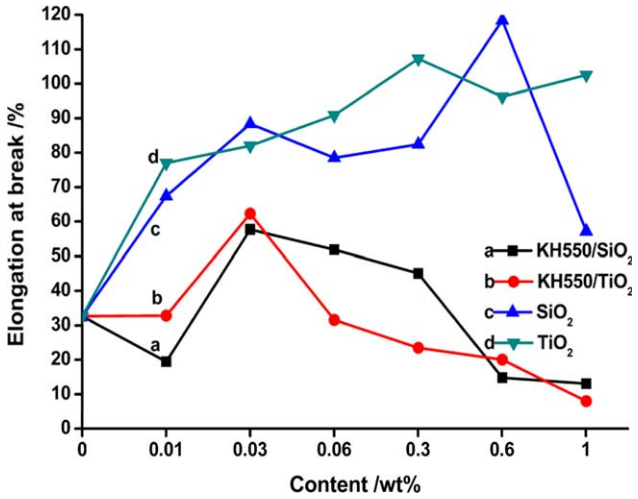

Figure 13. The effect of TiO_2 and SiO_2 content on elongation at break of silicone composites. [Color figure can be viewed in the online issue, which is available at wileyonlinelibrary.com.]

weakened by the coupling agent. The electrons within the composite would be distributed evenly under an electric field owing to the strongly enhanced interfaces between treated nanoparticles and the phenyl silicon rubber matrix.[28] In addition, the volume resistivity (ρ_v) of phenyl silicone rubber which blend with the untreated and treated nanoparticle maintain a similar trend.

Effect of SiO_2/TiO_2 Nanoparticles on Thermal Conductivity of Phenyl Silicone Rubber

The thermal conductivity as a function of nanofiller concentration for a silicone rubber containing either of the two fillers is shown in Figure 11. For both types of nanoparticles, the same increasing trend in conductivity is observed, which could be attributed to the large specific surface area of nanoparticle phases increasing photon scattering and improving thermal resistance. With an increase in the content of nanoparticles, the nanoparticles become more closely distributed throughout the polymer. This creates a network that promotes thermal conductivity in the composite as a whole. However, at the examined loading values, the thermal conductivity was not significantly improved. This could indicate that the distribution of the filler in the polymer matrix formed islands. The polymer is the continuous phase while the filler is dispersed phase, the filler is coated with the polymer matrix, which is similar to the "sea-island" two-phase structure in the polymer blends. Therefore, the particles cannot form a true thermal conductivity network, which requires intimate contact. It is readily observed that the thermal conductions of silicone rubbers treated with SiO_2 are higher than TiO_2, which is probably because the thermal conductivity of nano-SiO_2 (27 W/(m K)) is larger than nano-TiO_2 (1.8 W/(m K)). Furthermore, the thermal conductivity of treated nanocomposites is higher than the untreated nanocomposites under the same content.

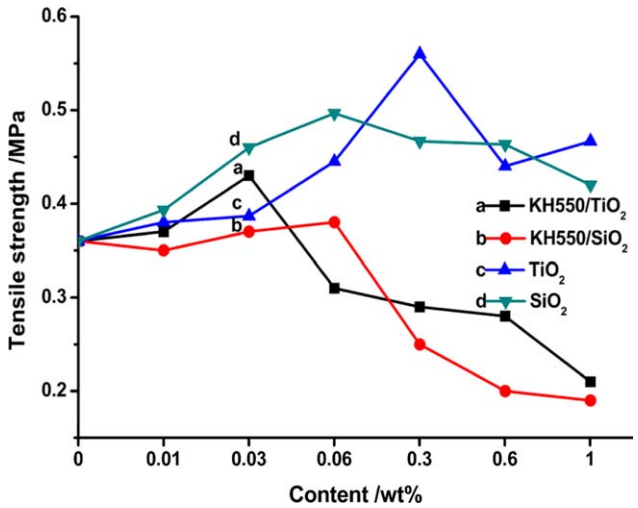

Figure 12. The effect of TiO_2 and SiO_2 content on tensile strength of silicone composites. [Color figure can be viewed in the online issue, which is available at wileyonlinelibrary.com.]

Measurements of Mechanical Properties

The mechanical properties of RTV silicones incorporated with TiO_2 or SiO_2 nanoparticles were tested, and the results are shown in Figure 12 (tensile strength) and Figure 13 (elongation at break).

As shown in Figure 12(curve a), the tensile strength of phenyl silicone rubber composites initially increases from 0.36 MPa to 0.43 MPa and then, decreases with increased loading of treated TiO_2. The dependence of tensile strength on the content of treated SiO_2 also follows this trend, as shown in Figure 12(curve (curve b). Similar responses could be obtained for untreated nanoparticles/silicone rubber composites (Figure 12, curve c, d).

As shown in Figure 13, the elongation at break initially increases with TiO_2 and SiO_2 content, and then reaches a maximum value. After this point, increasing the nanoparticle content results in a gradual decreased in elongation.

Compared to unfilled silicone composites, the addition of an appropriately chosen concentration of nanoparticles can improve the tensile strength and the elongation at break. This

Table I. Mechanical Properties of the Samples and Their Standard Deviations

Content (wt %)	Sample	Strength (N/mm^2)	Elongation at break (%)
0		0.36 ± 0.040[a]	33 ± 5.6
0.01	KH550/SiO_2	0.35 ± 0.045	20 ± 6.8
	KH550/TiO_2	0.37 ± 0.015	33 ± 3.1
	SiO_2	0.39 ± 0.061	67 ± 3.8
	TiO_2	0.38 ± 0.065	77 ± 6.8
0.03	KH550/SiO_2	0.37 ± 0.051	58 ± 8.3
	KH550/TiO_2	0.43 ± 0.026	62 ± 9.7
	SiO_2	0.46 ± 0.021	88 ± 7.2
	TiO_2	0.39 ± 0.009	82 ± 8.3
0.06	KH550/SiO_2	0.38 ± 0.095	52 ± 3.9
	KH550/TiO_2	0.31 ± 0.048	32 ± 8.4
	SiO_2	0.50 ± 0.043	79 ± 13
	TiO_2	0.45 ± 0.005	90 ± 3.3
0.3	KH550/SiO_2	0.25 ± 0.012	45 ± 2.8
	KH550/TiO_2	0.29 ± 0.046	24 ± 7.6
	SiO_2	0.47 ± 0.012	82 ± 8.6
	TiO_2	0.56 ± 0.073	107 ± 9.8
0.6	KH550/SiO_2	0.2 ± 0.025	15 ± 4.3
	KH550/TiO_2	0.28 ± 0.015	20 ± 8.2
	SiO_2	0.47 ± 0.057	118 ± 11
	TiO_2	0.44 ± 0.029	96 ± 13
1	KH550/SiO_2	0.19 ± 0.048	13 ± 5.7
	KH550/TiO_2	0.21 ± 0.053	8.0 ± 5.5
	SiO_2	0. 42 ± 0.052	57 ± 11
	TiO_2	0.47 ± 0.070	102 ± 8.7

[a] The numbers have been calculated by:, in this equation N, x_i, and $\bar{x}$ are the number of samples, the property for sample i, and the average property, respectively.

can be explained by physical and/or chemical reactions between the nanoparticles and the polymer chains. The surface energy of the nanoparticles typically decreases upon treatment with the coupling agent. In addition, the coupling agent has functional groups that are more compatible with the phenyl silicone rubber matrix when compared to the bare nanoparticle surface. Therefore, stronger interactions between treated nanoparticles and the phenyl silicone rubber enable a better load transfer between the two phases of the composite. However, particle agglomeration tends to reduce the strength of the material by creating regions of concentrated stress, which decreases the tensile strength of the material (Table I).[29]

CONCLUSION

In this article, the influences of SiO_2 and TiO_2 nanoparticles on properties of phenyl silicone rubber are investigated. The results indicate that the treated nanoparticles exhibit better compatibility with the matrix when compared to their untreated counterparts. Moreover, treated TiO_2 plays a more significant role in enhancing the UV-shielding ability of the phenyl silicone rubber, while treated SiO_2 has a stronger influence over enhancing the transmittance of visible light.

At first, the dielectric constant of nanocomposites decreased, and then it increased with the content of nanoparticles. Increasing the loading of nanoparticles results in a linear response in the thermal conductivity of both treated and untreated nanocomposites. The treated SiO_2 consistently provides the most improvement in thermal conductivity of the phenyl silicone rubber over the concentrations examined.

With an increase in the loading amount of nanoparticles, the tensile strength of the treated and untreated nanocomposites initially increased and then decreased.

REFERENCES

1. Osman, M. A.; Atallah, A.; Muller, M.; Suter, U. W. *Polymer* **2001**, *42*, 6545.
2. Joshi, V.; Srividhya, M.; Dubey, M.; Ghosh, A. K.; Saxena, A. *J. Appl. Polym. Sci.* **2013**, *130*, 92.
3. Saxena, A.; Dasgupta, D.; Bhat, S.; Tiwari, S.; Samantara, L.; Wrobel, D. *J. Appl. Polym. Sci.* **2014**, 131.
4. Bokobza, L. *J. Appl. Polym. Sci.* **2004**, *93*, 2095.
5. Dang, Z. M.; Xia, B.; Yao, S. H.; Jiang, M. J.; Song, H. T.; Zhang, L. Q.; Xie, D. *Appl. Phys. Lett.* **2009**, *94*, 042902.
6. Carpi, F.; De Rossi, D. *IEEE Trans. Dielect. Elect. Insul.* **2005**, *12*, 835.
7. Xu, J.; Wong, C. P. *Appl. Phys. Lett.* **2005**, *87*, 082907.
8. Zhuang, J.; Liu, P.; Dai, W.; Fu, X.; Lin, H.; Zeng, W.; Liao, F. *Int. J. Appl. Ceram. Technol.* **2009**, *7*, E46.
9. Di, M.; He, S.; Li, R.; Yang, D. *Nucl. Instrum. Meth. B* **2006**, *252*, 212.
10. Tuncer, E.; Sauers, I.; James, D. R.; Ellis, A. R.; Paranthaman, M. P.; Goyal, A.; More, K. L. *Nanotechnology* **2007**, *18*, 325704.
11. Kickelbick, G. *Prog. Polym. Sci.* **2003**, *28*, 83.
12. Paul, D. R.; Mark, J. E. *Prog. Polym. Sci.* **2010**, *35*, 893.
13. Iijima, M.; Omori, S.; Hirano, K.; Kamiya, H. *Adv. Powder Technol.* **2013**, *24*, 625.
14. Yilgor, E.; Eynur, T.; Kosak, C.; Bilgin, S.; Yilgor, I.; Malay, O.; Menceloglu, Y.; Wilkes, G. L. *Polymer* **2011**, *52*, 4189.
15. Le Strat, D.; Dalmas, F.; Randriamahefa, S.; Jestin, J.; Wintgens, V. *Polymer* **2013**, *54*, 1466.
16. Liu, B. T.; Tang, S. J.; Yu, Y. Y.; Lin, S. H. *Colloid Surf. A* **2011**, *377*, 138.
17. Nussbaumer, R. J.; Caseri, W. R.; Smith, P.; Tervoort, T. *Macromol. Mater. Eng.* **2003**, *288*, 44.
18. Ruiterkamp, G. J.; Hempenius, M. A.; Wormeester, H.; Vancso, G. J. *J. Nanopart. Res.* **2010**, *13*, 2779.
19. Lin, J.; Siddiqui, J. A.; Ottenbrite, R. M. *Polym. Adv. Technol.* **2001**, *12*, 285.
20. Mo, S. D.; Ching, W. *Phys. Rev. B* **1995**, *51*, 13023.
21. Ouyang, G.; Wang, K.; Chen, X. Y. *J. Micromech. Microeng.* **2012**, *22*, 074002.

22. Novak, B. M. *Adv. Mater.* **1993**, *5*, 422.
23. Yu, D. M.; Wu, J. S.; Zhou, L. M.; Xie, D. R.; Wu, S. Z. *Compos. Sci. Technol.* **2000**, *60*, 499.
24. Tsangaris, G. M.; Psarras, G. C.; Kouloumbi, N. *J. Mater. Sci.* **1998**, *33*, 2027.
25. Brosseau, C.; Quéffélec, P.; Talbot, P. *J. Appl. Phys.* **2001**, *89*, 4532.
26. Sawa, F. In IEEE Revealed Annual Conference on Electrical Insulation and Dielectric Phenomena, Vancouver, Canada, Oct 14–17, 2007; IEEE: New York, **2007**.
27. Picu, R.; Rakshit, A. *J. Chem. Phys.* **2007**, *126*, 144909.
28. Dang, Z. M.; Xia, Y. J.; Zha, J. W.; Yuan, J. K.; Bai, J. *Mater. Lett.* **2011**, *65*, 3430.
29. Huang, H. X.; Zhang, J. J. *J. Appl. Polym. Sci.* **2009**, *111*, 2806.